

Article

Analysis and Simulation of Adsorption Efficiency of Herbicides Diuron and Linuron on Activated Carbon from Spent Coffee Beans

Luiz Eduardo Zani de Moraes ¹, Felipe Augusto Olivo Marcoti ¹, Marco Antônio Naves Lucio ¹, Bianca Caroline da Silva Rocha ¹, Lucas Bonfim Rocha ² , Adriano Lopes Romero ³, Evandro Bona ⁴ , Ana Paula Peron ^{5,6}  and Osvaldo Valarini Junior ^{4,*} 

¹ Academic Department of Food and Chemical Engineering (DAAEQ), Federal Technological University of Paraná, Campo Mourão 87301-899, PR, Brazil; luizm.2002@alunos.utfpr.edu.br (L.E.Z.d.M.); felipemarcoti@alunos.utfpr.edu.br (F.A.O.M.); marcolucio@alunos.utfpr.edu.br (M.A.N.L.); biancacarolinerocha@alunos.utfpr.edu.br (B.C.d.S.R.)

² Department of Chemical Engineering, Federal Technological University of Paraná, Londrina 86036-370, PR, Brazil; lucasrocha@utfpr.edu.br

³ National Water Resources Management and Regulation Network (PROFÁGUA), Campo Mourão 80230-901, PR, Brazil; adrianoromero@utfpr.edu.br

⁴ Postgraduate Program in Food Technology (PPGTA), Federal Technological University of Paraná, Campo Mourão 80230-901, PR, Brazil; ebona@utfpr.edu.br

⁵ Graduate Program in Technological Innovations, Federal Technological University of Paraná, Campo Mourão 87301-899, PR, Brazil; anaperon@utfpr.edu.br

⁶ Graduate Program in Environmental Engineering, Federal Technological University of Paraná, Francisco Beltrão 85602-863, PR, Brazil

* Correspondence: osvaldovalarini@utfpr.edu.br; Tel.: +55-44-3518-1430

Abstract: Phenyl urea herbicides such as diuron and linuron are commonly used in agriculture to eliminate weeds. Their uncontrolled use can cause environmental problems. In this study, the adsorption of these herbicides was evaluated using activated carbon from coffee grounds, activated with zinc chloride (AC-ZnCl₂, 100% purity), nitric acid (AC-HNO₃, 65% purity), and commercially activated (AC-C) carbon for comparison purposes. The spent coffee grounds were transformed into activated carbon through the calcination process. The highest removal efficiency for diuron 40 mg·L⁻¹ and linuron 31 mg·L⁻¹ was obtained using the ZnCl₂-activated adsorbent, being 100% and 45%, respectively. The best pH range was between 4 and 6. Adsorption kinetic studies showed that pseudo-first and second-order models fit the experimental data, with the adsorption rate increasing rapidly within 60 min for the concentrations tested. Adsorption isotherms indicated that the Langmuir model provided the best fit for diuron, while the Freundlich model was more appropriate for linuron. The efficiency of the adsorption process using activated carbon (AC) was confirmed by the toxicity analysis of diuron and linuron solutions before and after adsorption with AC.

Keywords: activated carbon; toxicity of herbicides; isotherms and kinetics of adsorption; sustainability; activated carbon with ZnCl₂



Citation: Moraes, L.E.Z.d.; Marcoti, F.A.O.; Lucio, M.A.N.; Rocha, B.C.d.S.; Rocha, L.B.; Romero, A.L.; Bona, E.; Peron, A.P.; Junior, O.V. Analysis and Simulation of Adsorption Efficiency of Herbicides Diuron and Linuron on Activated Carbon from Spent Coffee Beans. *Processes* **2024**, *12*, 1952. <https://doi.org/10.3390/pr12091952>

Received: 31 July 2024

Revised: 30 August 2024

Accepted: 11 September 2024

Published: 11 September 2024



Copyright: © 2024 by the authors. Licensee MDPI, Basel, Switzerland. This article is an open access article distributed under the terms and conditions of the Creative Commons Attribution (CC BY) license (<https://creativecommons.org/licenses/by/4.0/>).

1. Introduction

Global herbicide production has been increasing by approximately 11% annually since 2017. Agricultural pesticides, such as herbicides, fungicides, and insecticides, have various social and environmental impacts. The uncontrolled use of these compounds can lead to resistance in target organisms, raising significant public health concerns due to their adverse effects on different species [1]. Herbicides can penetrate soils, potentially contaminating groundwater, and when leached into water resources, they can negatively impact various aquatic species [2].

Among the herbicide classes are phenyl urea types, such as diuron and linuron. Diuron, widely used worldwide, is applied in the cultivation of asparagus, grapes, cotton, fruits, and cereals and for algae control in fish production tanks [3]. In mammals, concentrations greater than $0.5 \mu\text{g}\cdot\text{L}^{-1}$ can cause cytogenetic, embryotoxic, and immunotoxin effects, endocrine disruption, and respiratory and cardiovascular problems [3]. Diuron is soluble in water, with a logarithmic octanol/water partition coefficient value of 2.60 [4]. Linuron, applied on broadleaf grasses like soybeans, corn, potatoes, and asparagus, was banned in the European Union, in 2017, due to its teratogenic and carcinogenic effects in mammals, causing infertility in women and low sperm production in men, along with toxicity to various aquatic organisms [5]. Soluble in water, linuron has a logarithmic octanol/water partition coefficient value of 3.00 and takes 60 days to degrade by half-life in soil [4,6].

In recent years, technologies have been developed to minimize or remove these herbicides from the environment since conventional techniques inefficiently remove such pollutants from water, such as physical or advanced chemical adsorption, photocatalytic degradation, chemical degradation, and biological treatments [3]. The adsorption process is effective for removing organic or ionic pollutants in inhomogeneous phases, with industrial waste used for the development of active carbon (AC) being widely employed [7].

AC is used for treating industrial waste and drinking water due to its high capacity to interact with organic pollutants in aqueous and gaseous environments. AC products are classified as granules, powder, and pellets based on their size and defined according to their porous structure: micro-, meso-, and macropores, correlated with their activation form: physical, chemical, and biological [8,9]. They are composed of the chemical compound carbon. Physical, chemical, and biological activations, mainly chemical, of the AC's surfaces are used to enhance the selectivity of functional groups such as carboxyl, carbonyl, phenols, quinones, and lactones [10,11].

Charcoal is an AC from environmental or industrial waste, such as sludge and forest residues, aimed at pollutant removal via adsorption processes [12]. Its production is similar to that of AC, but its physicochemical properties are modified to increase pollutant adsorption capacity [13]. One significant advantage of charcoal over AC is that industrial and environmental by-products can be economically reused and contribute to Sustainable Development Goals (SDGs) and circular economy precepts [13,14].

In this study, the AC was produced from spent coffee grounds, as coffee (*Coffea arabica*) is the second most traded commodity globally, with Brazil being the largest producer [15]. Approximately 170 million tons of coffee are produced per harvest, generating about 2.1 billion tons of spent coffee grounds [16]. Coffee grounds contain approximately 50% carbon on their surface, with the rest similar to lignocellulosic materials. During pyrolysis processes, oxygen and hydrogen detach from the molecular structure of this material, are transformed into gases, and its surface becomes porous. Its adsorptive capacity depends on the physicochemical parameters of the process, such as activation type, pyrolysis time, and temperature [17,18]. In water resources, spent coffee grounds can be toxic to aquatic animals, mainly due to caffeine [19,20].

Milanković et al. [21] analyzed the effectiveness of coffee grounds in removing organophosphate pesticides such as malathion and chlorpyrifos, pharmaceutical residues such as amoxicillin, rhodamine B, ceftriaxone, and cationic dyes such as methylene blue. The study analyzed adsorption at different temperatures and used kinetic methods such as pseudo-first and second order, Elovich, and intraparticle diffusion. The study used Freundlich, Langmuir, Temkin, and Dubinin–Radushkevich isotherms. The results revealed that a complex adsorption process involving monolayer and multilayer adsorption on the heterogeneous surface of the material was influenced by temperature, affecting maximum capacities and interactions. The material concentration of $0.5 \text{ mg}\cdot\text{mL}^{-1}$ increased the adsorption capacities for both pesticides, while for methylene blue, the material concentration of $0.1 \text{ mg}\cdot\text{mL}^{-1}$ exhibited high adsorption capacities for methylene blue. The pharmaceutical residues showed high adsorption capacities, especially for rhodamine B, $8250 \text{ mg}\cdot\text{g}^{-1}$. The adsorbent was regenerated using at least 10 cycles without significantly impacting the

adsorption capacity. The results highlight the potential of the carbon material from coffee grounds as an efficient adsorbent for various contaminants, highlighting its promising role in environmental remediation efforts.

Milanković et al. [22] studied the interaction between spent coffee grounds and the organophosphate pesticides, malathion and chlorpyrifos, for their removal from water and fruits. The study used first- and second-order kinetic models and Langmuir and Freundlich isotherms to analyze the adsorption mechanism. The adsorption capacity was $16 \text{ mg}\cdot\text{g}^{-1}$ and $7.00 \text{ mg}\cdot\text{g}^{-1}$ for malathion and chlorpyrifos, respectively. The study also evaluated the thermodynamic model of the adsorption systems, which was exothermic for malathion and endothermic for chlorpyrifos. The study was completed by testing plant extracts and carrying out an eco-neurotoxicological evaluation, showing no more neurotoxicity after adsorption. Rosson et al. [23] used coffee grounds in the form of AC with a potassium hydroxide activator and two other AC-C to evaluate the adsorption capacity, kinetics, and isotherms of phenolic compounds according to the models of the previous study. The assessed components were personal care and pharmaceutical products. The removal rate was around 70% for personal care products and 95% for pharmaceutical products, and all compounds were removed with active carbon powder. Table 1 summarizes some physicochemical parameters of diuron and linuron with adsorbents via the adsorption processes.

Table 1. Linuron and diuron adsorption results.

Herbicide/Adsorbents	pH	Mass Carbon	C_0 ($\text{mg}\cdot\text{mL}^{-1}$)	Removal (%)	Ref.
Diuron/bottom ash waste (BAW-200)	2.0	10 mg	20	80	[24]
Diuron/carbon from <i>Hovenia dulcis</i>	6.0	$1 \text{ g}\cdot\text{L}^{-1}$	200	95	[25]
Diuron/diochar <i>Hovenia dulcis</i>	7.0	$1 \text{ g}\cdot\text{L}^{-1}$	50	60	[26]
Diuron/carbon activated cassava biomass (<i>Manihot esculenta</i>)	7.0	$0.5 \text{ g}\cdot\text{L}^{-1}$	50–200	68	[27]
Diuron/carbon activated	7.0	$1 \text{ g}\cdot\text{L}^{-1}$	13–38	93	[28]
Linuron/carbon activated NORIT A2	7.0	$0.08 \text{ g}\cdot\text{L}^{-1}$	5	93	[29]
Linuron/zeolite combined with activated carbon	6.3	$0.1 \text{ g}\cdot\text{L}^{-1}$	2 ppm	77	[30]
Linuron/modified sludge-based biochar	7.0	$0.075 \text{ g}\cdot\text{L}^{-1}$	10	90	[31]
Linuron/hydrothermal treatment with FeOPa_{12}	7.6	$0.2 \text{ g}\cdot\text{L}^{-1}$	5	83	[32]
Linuron/chitosan and chitin	5.5	25 mg	10	12.5	[33]

C_0 = initial concentration.

Given the presented facts and the data in Table 1, using spent coffee grounds as AC for diuron and linuron adsorption introduces new parameters to the herbicide/adsorbent adsorptive process. This configuration makes the study of significant economic interest, as health and environmental problems are associated with the uncontrolled use of these herbicides and coffee waste. Therefore, this study aimed to evaluate diuron and linuron removal, kinetics, and adsorption isotherms using AC products. To confirm the efficiency of the evaluated adsorbents, a toxicity analysis of linuron and diuron solutions was conducted before and after adsorption on a widely used biological model in environmental impact studies.

The chemical compounds diuron, 3-3,4-dichlorophenyl-1,1-dimethylurea (chemical formula: $\text{C}_9\text{H}_{10}\text{Cl}_2\text{N}_2\text{O}$; molecular weight: $233.1 \text{ g}\cdot\text{mol}^{-1}$; molar volume: $170.1 \text{ cm}^3\cdot\text{mol}^{-1}$; pKa: 3.7; solubility of diuron in water is $42 \text{ mg}\cdot\text{L}^{-1}$ at 298 K) [27], and linuron, 3-3,4-dichlorophenyl-1-methoxy-1-methylurea (chemical formula: $\text{C}_9\text{H}_{10}\text{Cl}_2\text{N}_2\text{O}_2$; molecular weight: $249.09 \text{ g}\cdot\text{mol}^{-1}$; molar volume: $170.1 \text{ cm}^3\cdot\text{mol}^{-1}$; pKa: 3.7; solubility of linuron in water is $75 \text{ mg}\cdot\text{L}^{-1}$ at 298 K) [4].

2. Materials and Methods

2.1. Chemicals and Materials

The diuron and linuron were acquired from Sigma-Aldrich (San Louis, MO, USA) in analytical grade, i.e., 100% purity. Tween 80 purchased from Sigma-Aldrich (San Louis, MO, USA) in analytical grade, i.e., 100% purity, quantitative filter paper 7.5 microns Prolab (Sao Paulo, Brazil), zinc chloride (ZnCl_2), in analytical grade, i.e., 100% purity, nitric acid (HNO_3), in analytical grade, 65% purity and powdered activated carbon, in analytical grade, 100% purity, were also used, acquired from Dinamica (São Paulo, Brazil). A Brazilian agro-industrial cooperative (Coamo, Sao Paulo, Brazil) donated the spent coffee grounds. The equipment used included a Mettler Toledo balance (Sao Paulo, Brazil), Coel muffle furnace (Sao Paulo, Brazil), UV-VIS Global Analyzer Brazil spectrophotometer and Tecnal TE-4200 Shaker (Sao Paulo, Brazil).

Diuron and linuron have limited solubility in water. Thus, the stock solution for the removal efficiency analysis (%) was prepared by precisely dissolving $40 \text{ mg}\cdot\text{L}^{-1}$ of diuron [24] and $31 \text{ mg}\cdot\text{L}^{-1}$ of linuron [34] in deionized water with the addition of 1% Tween 80. This addition was necessary to solubilize the herbicide in solution. Subsequently, batch adsorption experiments in 50 mL were conducted in pH solutions of 2, 4, 6, 8, and 10 adjusted with HCl or NaOH to $0.1 \text{ mol}\cdot\text{L}^{-1}$. The adsorbent dosage was $100 \text{ mg}\cdot\text{L}^{-1}$ for both tested herbicides. For kinetic tests and to obtain adsorption isotherms, the solutions were diluted to the desired concentrations for model evaluation, and the optimal pH was chosen. All preparations were performed in triplicate.

2.2. Production of the ACs

The adsorbent mass was prepared by adding a 1:2 ratio of ZnCl_2 and HNO_3 , 65% purity, to spent coffee grounds in 60 mL of deionized water. This system was agitated at 50 rpm for 7 h at 85°C . Subsequently, the temperature was increased to 110°C until complete activation for 24 h. After this period, the moisture of the spent coffee grounds was stabilized in a muffle furnace at 600°C ; the spent coffee grounds were calcined, and inert gas N_2 was used at a flow rate of $1 \text{ mL}\cdot\text{min}^{-1}$ to maintain pore opening of the AC. Finally, the AC was washed with a 0.1 M HCl solution for 20 min and then with deionized water for the same period at a temperature of 85°C . To stabilize the zero charge point of the AC, the washing was completed with deionized water at room temperature ($T \cong 25^\circ\text{C}$), the relative humidity was stabilized, and the AC mass was separated into 100 mesh sieves for the adsorption tests in this study [16]. In the study by Rocha et al. [16], the relative humidity, the amount of ash, and the volatile compounds related to transforming the natural material into functional material were analyzed to find an average value with non-significant random and experimental error. This was performed to achieve greater purity, control the production process of adsorbent formation, and standardize the surface area, pore volume, functional groups, and isoelectric point of the AC produced. For all stages of AC production, procedures were performed in triplicate so as not to affect the reported parameters of the functional material [35,36].

Adsorption tests were carried out on powdered commercial carbon (AC-C) CAS: 7440-44-0. This coal has a BET (Brunauer-Emmett-Teller) surface area of $543.4 \text{ m}^2\cdot\text{g}^{-1}$ and a particle size between 1.4 and 2 mm [37]. That produced by spent coffee grounds activated with ZnCl_2 (AC- ZnCl_2) had an area of $564.4 \text{ m}^2\cdot\text{g}^{-1}$, pore volume of $0.32 \text{ cm}^3\cdot\text{g}^{-1}$, and micropore volume of $0.25 \text{ cm}^3\cdot\text{g}^{-1}$ and was activated with nitric acid, 65% purity (AC- HNO_3), 1.984 and micropore volume less than 0.01 [16].

2.3. Adsorption

The removal (%) was determined by evaluating the pH interference using a 50 mL aliquot of the stock solution under the described conditions. This aliquot was put into contact with AC-C for control, and AC- ZnCl_2 and AC- HNO_3 . The absorbance of diuron was measured at 247 nm [34] and linuron at 246 nm [22] using the UV-VIS Brazilian global analyzer spectrophotometer. For the herbicide, adsorbent systems were agitated in a Tecnal

TE-4200 Shaker for 24 h at $T = 25\text{ }^{\circ}\text{C}$ and 50 rpm. The pH levels were adjusted during adsorption by adding 0.1 M HCl and 0.1 M NaOH solutions, removing an aliquot of the samples every 3 h, and checking their value during adsorption [24,38]. Subsequently, the solution was filtered through 7.5 microns quantitative filter paper to separate the adsorbent from the solution, and the absorbance of each sample was measured. All sample studies were performed in triplicate, and the removal fraction was calculated according to (Equation (1)).

$$\text{Removal (\%)} = \left(1 - \frac{C_{\text{Final}}}{C_0}\right) \times 100. \quad (1)$$

C_{Final} represents the final concentration in $\text{mg}\cdot\text{L}^{-1}$ calculated from the calibration curve, and C_0 represents the initial concentration, $40\text{ mg}\cdot\text{L}^{-1}$ for diuron and $31\text{ mg}\cdot\text{L}^{-1}$ for linuron. The adsorption kinetics were conducted, and the optimal pH condition was selected under the same conditions as the removal (%) experiment. All tests were carried out in triplicate, and the adsorbent material was uniform in 10 mesh sieves, and temperature and agitation were controlled so as not to interfere with removing the herbicide [35,36].

Aliquots of the solution were withdrawn at 15 and 1440 min and measured in the spectrophotometer. The experimental values were determined by (Equation (2)).

$$Q_e = \frac{(C_0 - C_e)}{m} \times V \quad (2)$$

where Q_e is the mass adsorption capacity at equilibrium ($\text{mg}\cdot\text{g}^{-1}$), C_e is the pollutant concentration at equilibrium ($\text{mg}\cdot\text{g}\cdot\text{L}^{-1}$), V (L) is the volume of the solution, and m (mg) is the mass of the adsorbent. The models used to fit a system to the experimental data are the pseudo-first-order model (Equation (3)) and the pseudo-second-order model (Equation (4)) [39,40].

$$\frac{dQ}{dt} = k_1 \times (Q_e - Q_t) \quad (3)$$

$$\frac{dQ}{dt} = k_2 \times (Q_e - Q_t)^2 \quad (4)$$

where Q_t is the total mass adsorption capacity of the pollutant at a given time ($\text{mg}\cdot\text{g}^{-1}$), and k_1 (min^{-1}) and k_2 ($\text{g}\cdot\text{mg}^{-1}\cdot\text{min}^{-1}$) are the kinetic constants of the tested models.

The adsorption isotherms were analyzed for concentrations of 5, 10, 20, 50, and $70\text{ mg}\cdot\text{L}^{-1}$ in deionized water solutions with 1% Tween 80 under the same conditions as the previous experiments. Such analysis is necessary to determine the adsorbate relationship in the adsorption–desorption equilibrium solution. After reaching equilibrium after 24 h, the samples were filtered, and the concentrations of diuron and linuron were determined using (Equation (2)). The isotherm models tested for these data were the Langmuir model (Equation (5)) and the Freundlich model (Equation (6)).

$$Q_e = \frac{Q_{\text{max}} \times K \times C_e}{1 + K \times C_e} \quad (5)$$

$$Q_e = K_F \times C^{1/n} \quad (6)$$

where Q_{max} represents the adsorption capacity of the adsorbent at a given equilibrium concentration ($\text{mg}\cdot\text{g}^{-1}$), K is defined as the affinity between the adsorbate and the adsorbent ($\text{L}\cdot\text{mg}^{-1}$), K_F is defined as the intensity of adsorption ($\text{mg}\cdot\text{g}^{-1}\cdot\text{L}^{-1}$), and n is related to the energetic surface of adsorption. The Langmuir model describes adsorption phenomena on energetically homogeneous surfaces [41], while the Freundlich model describes heterogeneous surfaces.

The regeneration protocol was performed after the completion of the adsorption process after the kinetic process of diuron and linuron [21,24]. The functional material was collected, centrifuged, and washed, and then 30 mL of analytical grade ethanol, purity,

99.6%, was added at 20 ± 1 °C for 5 h to desorb diuron and linuron. Finally, the sorbent was washed with deionized water for reuse over 5 cycles.

2.4. Evaluation of the Phytotoxic, Cytotoxic, and Genotoxic Potential of Diuron and Linuron in Aqueous Medium before and after Adsorption with AC on *Allium cepa* L. (Onion) Roots

Toxicity tests on *A. cepa* roots were conducted to assess and compare the efficiency of AC in removing diuron and linuron from the aqueous medium.

A linuron solution of $31 \text{ mg}\cdot\text{L}^{-1}$ and a diuron solution of $40 \text{ mg}\cdot\text{L}^{-1}$ were prepared for the tests. These concentrations were prepared in a deionized water solution with 1% Tween 80.

The *A. cepa* bulbs were obtained from an organic garden and were free from pesticides and synthetic fertilizers. After removing the dry cataphylls, the bulbs were washed in deionized water. Subsequently, onions were placed in contact with the following treatments (for each treatment, five onion bulbs were used): diuron solution at a concentration of $40 \text{ mg}\cdot\text{L}^{-1}$; linuron solution at a concentration of $31 \text{ mg}\cdot\text{L}^{-1}$; diuron solution after adsorption with AC-C; linuron solution after adsorption with AC-ZnCl₂ and AC-HNO₃; linuron solution after adsorption with AC-C; linuron solution after adsorption with AC-ZnCl₂ and AC-HNO₃; distilled water (used as control). Immediately after, the onions in contact with their respective treatments were placed in a BOD incubator (Cinelab, Sao Paulo, Brazil) for 120 h, without light presence, for rooting.

The phytotoxicity, cytotoxicity, and genotoxicity tests on *A. cepa* roots were conducted according to [42]. For phytotoxicity analysis, 10 roots were measured from each bulb. Thus, for each treatment, a total of 50 roots were measured. Subsequently, each treatment's mean root length (ARL) was determined according to (Equation (7)). The roots were measured with a manual caliper. The results obtained from ARL for the control were considered 100%. Thus, data were expressed as a percentage of control values for the ARL of treatments.

$$ARL(cm) : \frac{\text{Sum of root length of root bundles}}{5} \times 100 \quad (7)$$

Root meristems were used for cytotoxicity and genotoxicity analyses. For this purpose, on average, three roots from each bulb were collected and placed in Carnoy fixative for 24 h. Subsequently, the roots were washed in distilled water, hydrolyzed in 1 N HCl for 8 min, and washed again. Afterward, the meristematic regions of the roots were dissected and crushed with a scalpel on glass slides, stained with 2% acetic orcein, and covered with a coverslip. The slides were analyzed under an optical microscope (Nikon, Sao Paulo, Brazil) with a 40× objective.

Cytotoxicity was determined by the mitotic index (MI), which was calculated according to (Equation (8)), where cells in interphase (cells that are not dividing) and cells in prophase, metaphase, anaphase, and telophase (cells that are dividing) were counted. From each bulb, 2000 cells were counted, totaling 10,000 cells analyzed per treatment. The results obtained from MI for the control were considered 100%. Thus, data were expressed as a percentage of control values for the MI of treatments.

$$MI : \frac{\text{Total number of dividing cells}}{\text{Total number of cells analyzed}} \times 100 \quad (8)$$

Genotoxicity was determined by the percentage of cellular changes (IAC). From each bulb, cells with alterations were analyzed, such as cells with micronuclei, cells with chromosomal bridges, and cells with chromosomal breakage. This analysis considered cells in interphase and cells undergoing division (prophase, metaphase, anaphase, and telophase). Two hundred cells from each bulb were analyzed, totaling 2000 cells analyzed for each treatment, as per (Equation (9)).

$$IAC : \frac{\text{Number of cellular alterations}}{\text{Total number of cells analyzed}} \times 100 \quad (9)$$

The toxicity results for the different treatments were evaluated using the Kruskal–Wallis et al. [43], analysis of variance, followed by the Dunn test ($p \leq 0.05$).

3. Results

3.1. Adsorption

The removal (%) was obtained from the experiments conducted to compare the herbicides and AC concerning pH.

Figure 1 shows diuron and linuron adsorption efficiency on AC-ZnCl₂, AC-HNO₃, and AC-C. For diuron (Figure 1a), the pH ranges from 2 to 10 had different adsorption percentages under the tests assessed. This could be associated with the surface area of the AC tested, as the volume of micropores is the primary variable defining the adsorption capacity of an AC. Another variable that may interfere with the adsorption capacity is the distribution of functional groups on its surface, as the variability of functional groups on the surface of the AC affects the binding mechanism between the pollutant and the adsorbent [16].

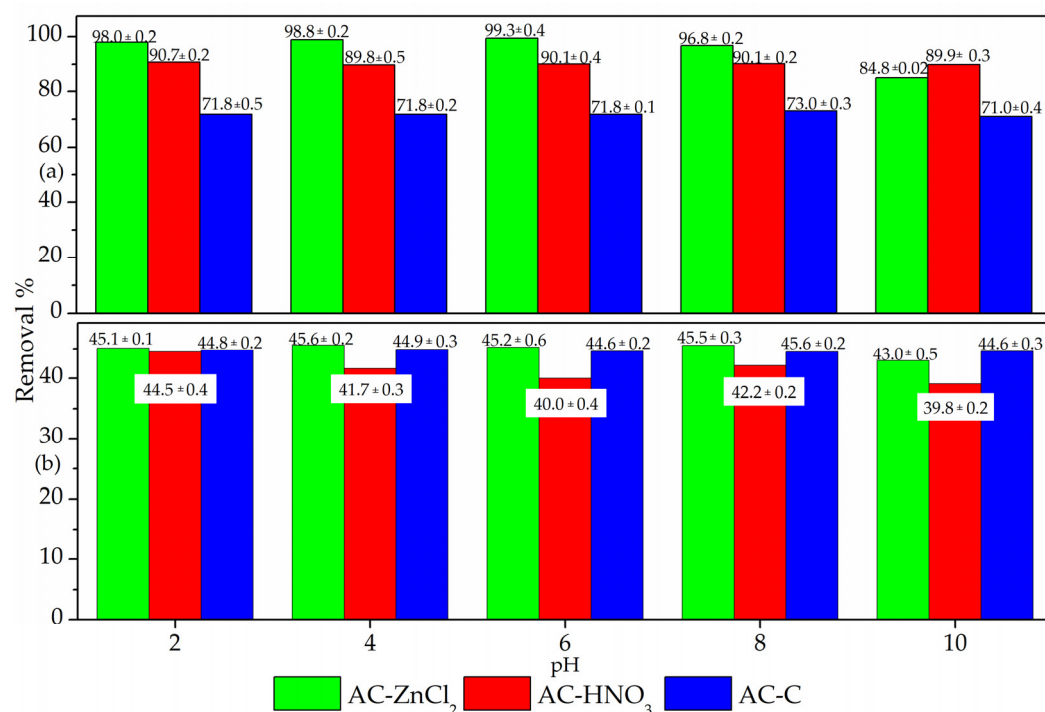


Figure 1. Removal (%) in different pH. (a) Diuron, (b) linuron.

The difference in removal (%) for linuron was not as pronounced (Figure 1b). It was also observed that the pH variation did not influence significant changes in removal (%). For the pollutant, the functional material systems are usually altered due to pH variation [44]. It was also noted that, for diuron, there was more significant adsorption compared to linuron, which may be due to the size of the molecules of the analyzed chemical compounds, Mw: 233.1 g·mol⁻¹ for diuron compared to Mw: 249.09 g·mol⁻¹ for linuron, and the physicochemical properties, ionic nature, and polarity of the chemical compounds interfered with adsorption [45]. The highest removal (%) values found for diuron and linuron were between pH 4 and 6, possibly due to the AC neutral charge point of 5.8.

The surfaces of AC can accommodate different elements, depending on the activation mode. In general, chemical activators such as ZnCl₂ and HNO₃ diversify oxygenated functional groups, such as carboxylic acids, hydroxyls associated with aromatic chains, carbonyls, lactones, and quinones [10,11,46]. The use of precursor and volatile materials, such as the one in this study, facilitates the diversification of functional groups and dehy-

dration of the lignocellulosic part of spent coffee grounds. The precursors increase the mass proportion and stimulate the release of volatile substances into the medium, consequently increasing the adsorbent's surface area.

Using chemical activators contributes to the formation of micro- and mesopores and better functional distribution on the surface of the functionalized material [46]. The most commonly used chemical activator is ZnCl_2 . Activation with ZnCl_2 induces an electrolytic action called swelling in the molecular structure of cellulose. This effect causes the breakdown of the cellulose molecules and increases different intra- and inter-coated cavities, which produce a greater surface area on the AC- ZnCl_2 [47]. This compound acts as a buffering agent for samples impregnated with this chemical activator, moving volatile substances through saturated ZnCl_2 due to its dehydrating effect on lignocellulosic materials when in contact. ZnCl_2 also contributes to the volatilization of substances impregnated with the functional material, forming a larger surface area and increasing the pore cavities [47]. The pores are not ruptured after activation with ZnCl_2 , and aromatic compounds with large rings are adsorbed more easily into the functional material AC- ZnCl_2 [48]. This compound does not react with carbon; the activated carbon obtained has a higher yield than activated carbon produced with another activator [49].

On the other hand, the activation with HNO_3 decreases the surface area, pore volume, and pore width compared to AC- ZnCl_2 . This situation was due to the introduction of functional groups into the activated carbon's pores and the aliphatic lower stability, which is oxidized, destroying the porous structure [50,51]. There is a decrease in pore width; the average size was still contained in the mesopore (2–50 nm). Thus, in this study, the activation of ZnCl_2 with coffee grounds became more effective than that of HNO_3 with coffee grounds and the AC-C under study. ZnCl_2 has a higher yield in breaking down cellulosic compounds than HNO_3 [47]. This causes the carbon to increase with the polymerization of aromatic compounds, facilitating the adsorption of pollutants [48]. This may be one of the factors that the surface area of this compound is more significant than AC- HNO_3 , $564 \text{ m}^2 \cdot \text{g}^{-1}$, compared to $1.984 \text{ m}^2 \cdot \text{g}^{-1}$ [16].

The interaction mechanisms of the adsorption process of the contaminant with the adsorbent were proposed to consider the reaction of radicals and non-radicals involved in the degradation of the pollutant, diuron or linuron, in the use of the functional material [16,33,44,52,53]. Thus, in an aqueous solution, the hydroxyl (OH^-) of water and the radicals (Cl^-) and (NO_3^-) of the chemical agents become ionized. The interactions of these radicals with the pollutants form intermediate products. This occurs due to the functional groups containing oxygen on the surface of the functional materials. For linuron, a mesomeric effect occurs in the double bond of carbon, where the double bond of carbon passes to the bond with the nitrogen attached to the aromatic ring, making the nitrogen cation and oxygen anion; then this interaction around carbon shifts to the nitrogen attached to CH_3 and OCH_3 [33]. This mesomeric effect causes adsorption between the molecule and the AC. For diuron, the same mechanism occurs. However, it also occurs around the carbon with a double bond. The OH^- groups contribute to redox reactions and electron transfer in mesomeric effects. The electrons from AC that interact with diuron and linuron increase the electron transfer capacity through π electrons, performing the adsorption process [52].

Figures 2 and 3 show the trend of the adsorption–desorption system of the analyzed chemical compounds.

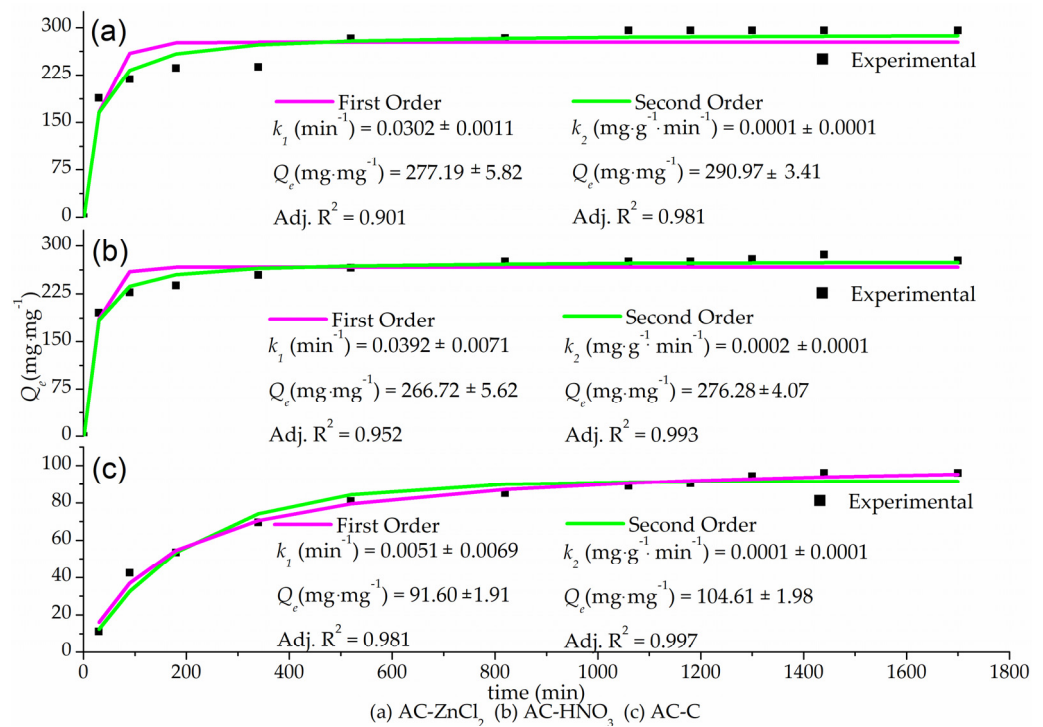


Figure 2. Kinetic parameters of diuron adsorption isotherms on AC. (a) AC-ZnCl₂. (b) AC-HNO₃, (c) AC-C.

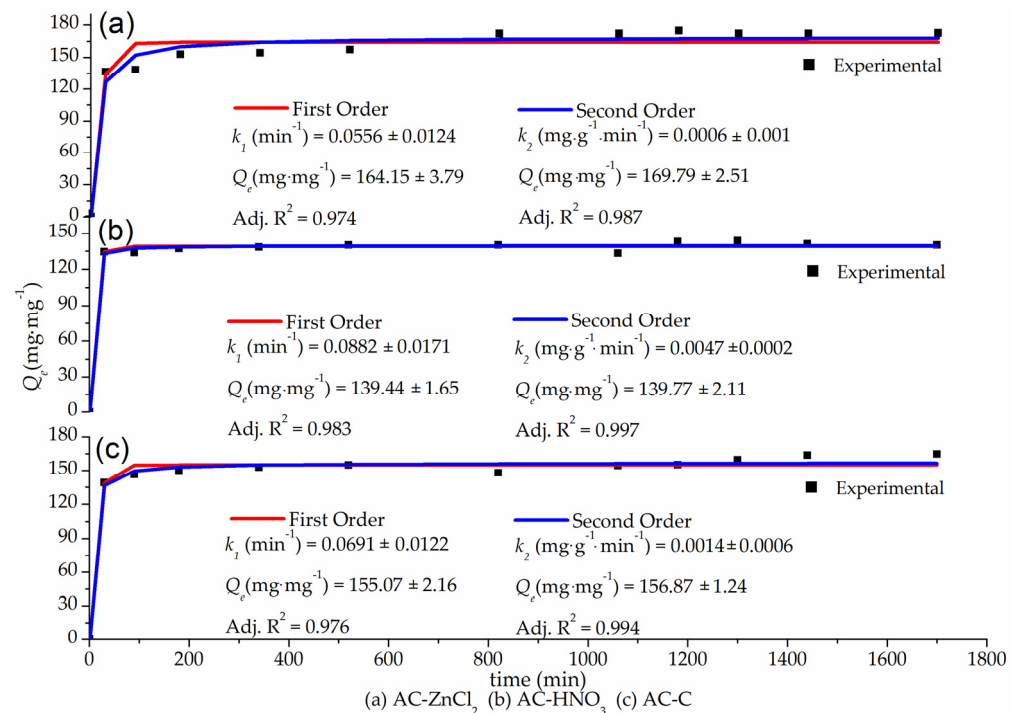


Figure 3. Kinetic parameters of linuron adsorption isotherms on AC. (a) AC-ZnCl₂. (b) AC-HNO₃, (c) AC-C.

The experimental data obtained were modeled using Equations (3) and (4), referring to the pseudo-first-order and pseudo-second-order models. The presented results show that diuron (Figure 2) and linuron (Figure 3) adsorption was relatively rapid for the three tested adsorbents. Adsorption–desorption equilibrium occurred around 60 min, except for the diuron AC-C system, which achieved a later adsorption–desorption equilibrium

around 1000 min. The maximum amount of diuron and linuron occurred with the AC-ZnCl₂ adsorbent. Fast and slow adsorptions occur because the available active sites for adsorption reach equilibrium, meaning that there are no more active sites to adsorb the chemical compound, achieving saturation of the adsorptive system. This occurs due to several factors, such as the polarity of the chemical compound, operating pH, temperature, and mainly the surface area of the adsorbent [16]. In adsorption processes, the fastest process occurs inside the pores through variables such as intraparticle diffusion and the concentration gradient of the chemical compound [54].

Figures 2 and 3 also present the kinetic parameters of the analyzed systems in this study. Based on the fitting models tested, for the pseudo-first-order model, the maximum adsorption quantity at equilibrium Q_e ($\text{mg}\cdot\text{g}^{-1}$), time t (min), and the rate constant of adsorption k_1 (min^{-1}) were calculated. The intraparticle diffusion rate constant k_2 ($\text{mg}\cdot\text{mg}^{-1}\cdot\text{min}^{-1}$) was calculated for the pseudo-second-order model [55]. From the coefficient of determination (adj. R^2), it was possible to describe the models based on experimental data. The model that best represented the experimental data was the pseudo-second-order model for all adsorbents. This model phenomenologically represents short-duration systems, the inverse of the first-order model [56]. The initial concentration chosen for the adsorption system can also interfere with kinetics. The pseudo-second-order model is more applied to the final phases of adsorption because this model is based on the rate-limiting step throughout the process, which is chemisorption. Thus, the adsorption rate depends on the adsorption capacity of diuron and linuron and not on its concentration [55]. Therefore, systems with higher adsorption capacity are chemical compounds and AC-ZnCl₂. Figures 4 and 5 show the equilibrium data of the herbicide and adsorbent systems.

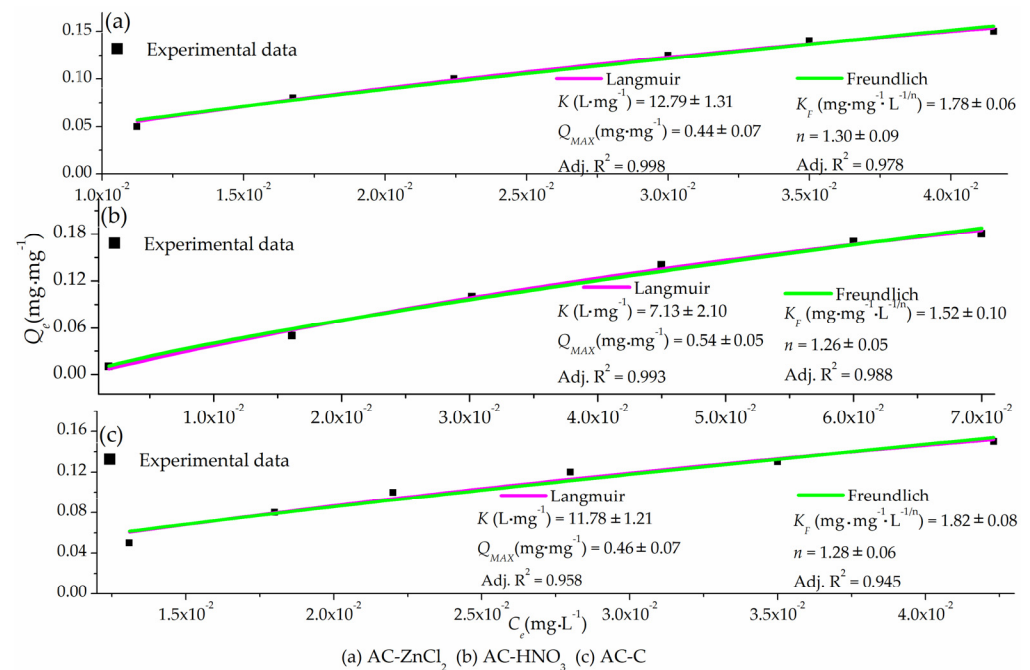


Figure 4. Diuron adsorption isotherms of AC products with C_0 ranging from 1×10^{-2} to 4×10^{-2} $\text{mg}\cdot\text{L}^{-1}$. (a) AC-ZnCl₂, (b) AC-HNO₃, and (c) AC-C.

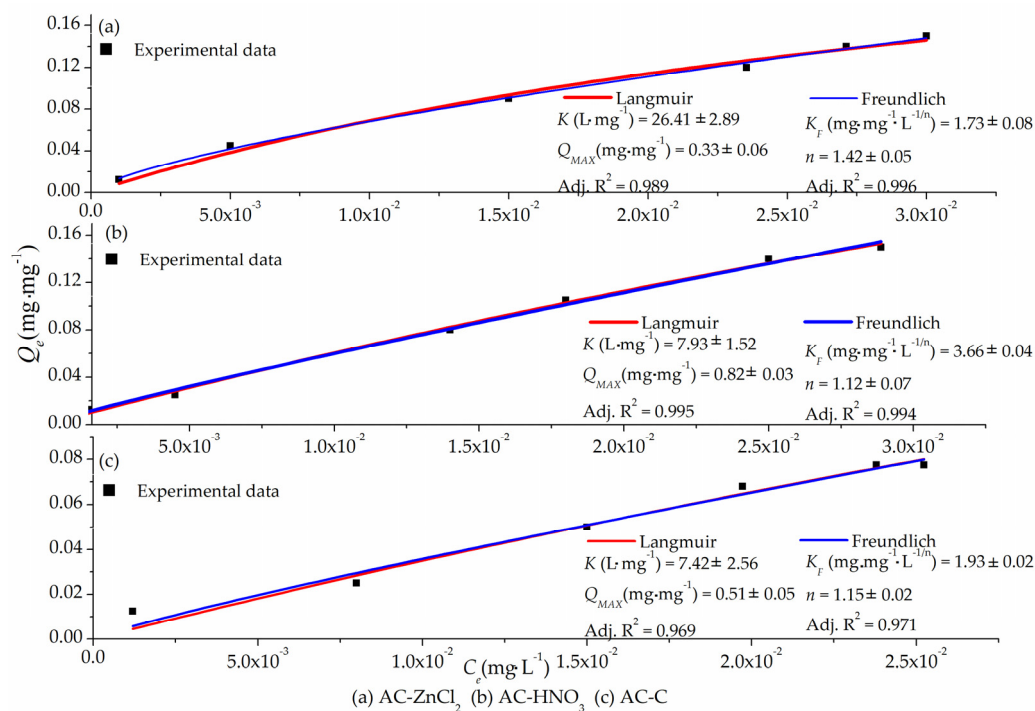


Figure 5. Linuron adsorption isotherms of AC products with C_0 ranging from 1×10^{-2} to 3×10^{-2} mg·L⁻¹. (a) AC-ZnCl₂, (b) AC-HNO₃, and (c) AC-C.

The equilibrium concentrations found occur after the 720 min interval. To optimize the use of adsorbents for adsorption processes, the adsorption isotherms of Langmuir (Equation (5)) and Freundlich (Equation (6)) were tested to describe how the pollutant concentration interacts with the surface of the adsorbent. Figures 4 and 5 show a favorable adsorption behavior of diuron and linuron in the tested concentration range. The experimental data indicate that the adsorption of diuron and linuron did not reach high levels. Figures 4 and 5 also show the simulated parameters of the Langmuir and Freundlich models [57].

For the herbicides, the adsorbent that best represented the models based on experimental data was AC-ZnCl₂. The Langmuir model obtained a better correlation for the diuron system and AC-ZnCl₂. The system shows that Q_{max} and K values were higher than AC-C. Q_{max} indicates that factors such as specific area, pore volume, pore size distribution, and multicamera development presented more beneficial results for the adsorption process, and high K indicates that the surface of the functional material has a higher affinity with diuron. The Langmuir model indicates that this system has homogeneous surfaces, allowing monolayer surface coverage of the adsorbents as ACs saturates [16]. This model also indicates that the process allows desorption. The Freundlich model had a higher adj. R^2 for the linuron system with AC-ZnCl₂. This model phenomenologically represents heterogeneous adsorbents and defines the distribution of active sites as exponential. The Freundlich model has the term n , which indicates that higher values show that the adsorption was carried out spontaneously [55].

Comparing the herbicide diuron with other adsorbents presented in Table 1, for Zbair et al. [24], who used ash residues, the removal efficiency was influenced by the pH, increasing linearly between pH 2 and 6, stabilizing at 80% for the other pHs. What may have interfered with the efficiency of this system is the isoelectric point of this adsorbent, which was 6.9; since diuron has a pKa of 3.7, considered very acidic, this ionic difference may decrease the removal efficiency due to the types of bonds made between the adsorbent and the herbicide. The amount of adsorbent in the herbicide was also evaluated, and as the amount of adsorbent increased, the removal efficiency decreased. The authors also found an adsorption capacity similar to this work at a temperature of 20 °C, and the most

efficient isotherm model was Langmuir. Georgin et al. [25] found the optimum condition of removal (%) and adsorptive capacity were close to 90% and $47 \text{ mg}\cdot\text{L}^{-1}$ for a $1.0 \text{ g}\cdot\text{L}^{-1}$ of activated carbon *Hovenia dulcis*. In their study, the authors observed that removal (%) was proportional to the increase in adsorbent, while the adsorption capacity was inversely proportional. The best isotherm fit was also the Langmuir isotherm.

Vieira et al. [26] used the adsorbent *Hovenia dulcis* by chemical activation with ZnCl_2 to adsorbent diuron. The study showed a removal efficiency of 60% at pH 7.0; the adsorption capacity increased with the temperature reaching $119.7 \text{ mg}\cdot\text{g}^{-1}$, and the increase in temperature indicates that the position of the molecule was parallel to the receptor sites, occupying more than one site at the same time with the temperature rise. The Langmuir model was also the one that best represented the system. Georgin et al. [27], using AC obtained from residual Cassava biomass (*Manihot esculenta*), observed that the increase in concentration in relation to the tested adsorbent increased the adsorption efficiency, which was 67%. The adsorption capacity was $166 \text{ mg}\cdot\text{g}^{-1}$ for the concentration of $200 \text{ mg}\cdot\text{L}^{-1}$, reaching equilibrium around 60 min. In this study, the isotherm fits the Freundlich model. From these results, the system developed for this study of diuron was efficient since a removal efficiency was more significant than those presented, and a high adsorption capacity was obtained, as some studies reported. This may be associated with the fact that coffee powder contains about 50% carbon; the original lignocellulosic materials have a similar composition: 49% C, 6% H, 0.2% N, and during carbonization most of the hydrogen and oxygen are lost [17] to the carbonization parameters [58], and the herbicide concentration–pollutant ratio [16,59].

From the perspective of comparing the linuron results from this study with those in Table 1, Elazabi et al. [29] used a concentration of $5 \text{ mg}\cdot\text{L}^{-1}$ with the adsorbent NORIT SA2 $0.08 \text{ g}\cdot\text{L}^{-1}$; the study obtained a removal efficiency close to 95% for all pHs 3–10 tested. The adsorption capacity found was $90 \text{ mg}\cdot\text{g}^{-1}$. The author observed that the increase in adsorbent about linuron did not increase the adsorption capacity. This can be justified by the number of sites available to adsorb the linuron molecule in solution. The linuron concentration is also eight times lower than used in this study, which may have increased the removal efficiency. Sirival et al. [30] synthesized zeolite with activated carbon to evaluate the removal of linuron. The removal efficiency was close to 77%, the adsorption capacity reached equilibrium at around 1440 min, and the Langmuir model was the most suitable for the adsorption process.

Yang et al. [31] evaluated the removal efficiency as a function of the agitation speed for linuron with modified sludge-based biochar. The efficiency increased to 220 rpm and remained stable up to 240 rpm. The adsorption capacity went from $4.5 \text{ mg}\cdot\text{L}^{-1}$ to $12 \text{ mg}\cdot\text{L}^{-1}$ when the concentration was changed from 10 to $20 \text{ mg}\cdot\text{L}^{-1}$. Finally, the pH from 3 to 10 did not affect the adsorption quantity of modified sludge-based biochar, and the most suitable model for the system was the Langmuir model. In the study by Belaroui et al. [32], the adsorption of linuron by an Algerian palygorskite modified with magnetic iron had the amounts of herbicide varied as magnetic palygorskite modified by magnetic iron oxides by thermal synthesis (83%), magnetic palygorskite modified by magnetic iron oxides (55%), magnetic palygorskite (27%). The initial concentration of the adsorbate and the effect of temperature influenced the removal efficiency. The best-adjusted adsorption isotherm was the Freundlich one.

Rissouli et al. [33] evaluated the removal of linuron using chitosan and chitin; the adsorption capacity was approximately $5 \text{ mg}\cdot\text{g}^{-1}$ for linuron/chitosan, being stabilized around 100 min, the pH influenced the removal capacity of the herbicide, and the Langmuir model was the most appropriate. Based on these studies for linuron, it can be observed that the system proposed in this study was not efficient in removal efficiency; however, in terms of adsorption capacity, the system was favorable.

Based on the facts presented, this study had the best result from the adsorbent AC- ZnCl_2 for both herbicides. Finally, the five regeneration cycles of this adsorbent were analyzed (Figure 6).

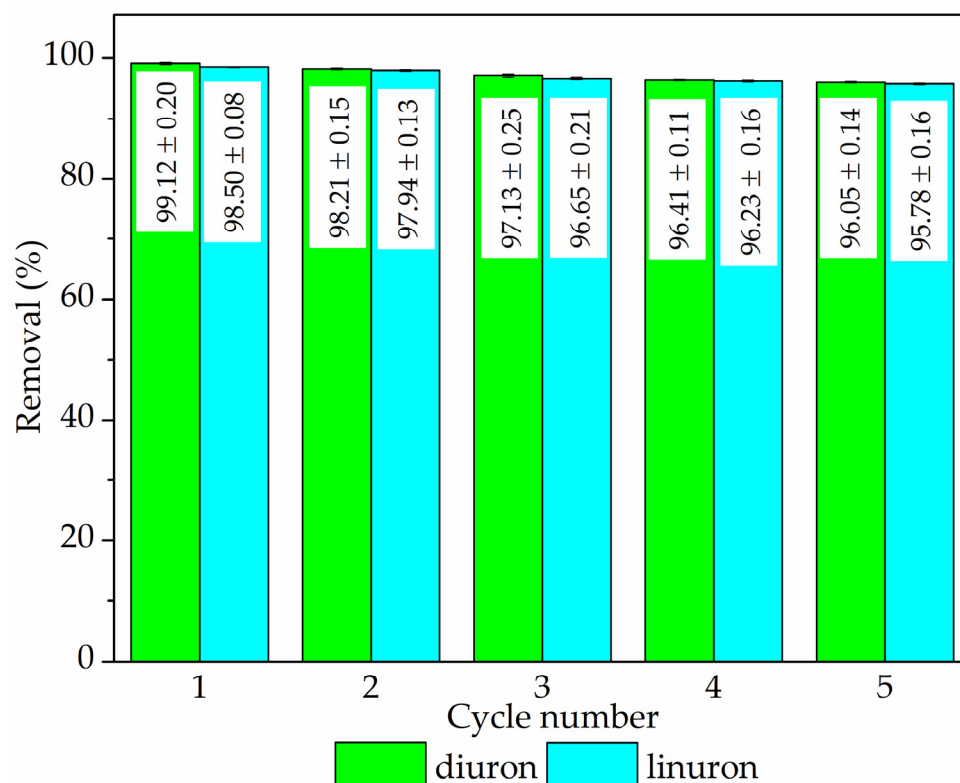


Figure 6. Regeneration and recyclability of AC-ZnCl₂ over five cycles of use.

To evaluate the regeneration and reuse of the AC-ZnCl₂ adsorbent, the adsorbed concentrations of contaminants were determined as previously described. The AC-ZnCl₂ showed a high removal efficiency after five stages of recycling. The removal proficiency of AC-ZnCl₂ in the first cycle was 99.12% ± 0.20%. From the first cycle onwards, there was a decrease in the removal proficiency. Still, it can be deduced that AC-ZnCl₂ has excellent desorption capacity and can be easily recycled from wastewater using ethanol as a solvent. By observing the results in Figure 6, it can be concluded that the material can be successfully regenerated using 5 mL of 25% ethanol solution and reused for at least five cycles without significant impact on the adsorption capacity. These results were similar to the studies of Zbair et al. [24] and Milanković et al. [21].

3.2. Toxicity

For over fifty years, *A. cepa* roots have been used worldwide to evaluate water resources' phytotoxic and cytogenetic potential, effluents from different sources, and environmental contaminants. Even when the concentration of these compounds in the environment is on the nanogram (ng) scale, they prove highly sensitive to xenobiotics [60,61]. The results obtained through this bioassay show a significant correlation with results obtained in other test systems, such as in animals, cell cultures, and other plants [61,62].

Table 2 shows that the solution of diuron at 40 mg·L⁻¹ and linuron at 31 mg·L⁻¹, before adsorption, significantly reduced root elongation. Furthermore, they caused disturbances in cell division by substantially decreasing the mitotic index in root meristems and induced the formation of significant alterations in meristematic cells. Based on these results, diuron and linuron at the evaluated concentrations caused phytotoxicity, cytotoxicity, and genotoxicity in *A. cepa* roots.

Table 2. The average growth and mitotic index of *Allium cepa* L. roots presented with diuron and linuron solutions.

TR	ARL/SD (%)	MI/SD (%)
Co	100 ± 1.0	100 ± 0.9
Diuron		
DS before adsorption	50.0 ± 1.3 *	52.0 ± 1.4 *
DS after adsorption with AC-C	90.4 ± 1.0	92.5 ± 1.5
DS after adsorption with ACs	97.9 ± 1.0	95.9 ± 1.1 *
Linuron		
LS before adsorption	52.8 ± 1.5 *	50.8 ± 1.0 *
LS after adsorption with AC-C	90.9 ± 1.5	90.5 ± 1.5
LS after adsorption with ACs	94.7 ± 0.9	97.9 ± 1.0

DS: diuron solution, LS: linuron solution TR: treatment, ARL: average root length, MI: mitotic index, SD: standard deviation, Co: control. For ARL and MI, data are expressed as a percentage of control values. * Significantly different from the Co, according to Kruskal–Wallis H followed by Dunn’s post hoc test ($p \leq 0.05$).

Many studies in the literature report the cytotoxicity and genotoxicity of linuron in different bioassays, such as in mammalian cell lines [63], in various tissues of rats [64], in gill and liver tissues of fish [65], and in root meristematic cells of *A. cepa* [66]. Similarly, studies have shown the cytogenotoxicity of diuron in diversified test systems [67,68], such as in sperm and embryos of oysters, in root meristematic cells of *A. cepa* [69], and *Drosophila melanogaster* L. [70]. The studies for diuron and linuron corroborated the toxicity results observed for these two herbicides before adsorption with AC (Tables 2 and 3).

Table 3. Number, types, and cellular alteration index in *A. cepa* bulb root meristem cells exposed to diuron and linuron solutions.

	Number and Types of Cellular Changes			
	Micronucleus	Chromosomal Bridges	Chromosomal Disruptions	CAI ± SD (%)
Co	3	0	0	0.15
DS before adsorption	78 *	44 *	87 *	10.45 *
DS after adsorption with AC-C	1	0	2	0.15
DS after adsorption with AC-ZnCl ₂	1	1	1	0.15
DS after adsorption with AC-HNO ₃	2	1	1	0.25
LS before adsorption	92 *	55 *	76 *	11.15 *
LS after adsorption with AC-C	1	1	4	0.30
LS after adsorption with AC-ZnCl ₂	1	1	0	0.10
LS after adsorption with AC-HNO ₃	1	1	1	0.15

DS: diuron solution, LS: linuron solution TR: treatment, CAI: cellular alteration index, SD: standard deviation, Co: control. For ARL and MI, data are expressed as a percentage of control values. * Significantly different from the Co, according to Kruskal–Wallis H followed by Dunn’s post hoc test ($p \leq 0.05$). AC-ZnCl₂ or AC-HNO₃.

In Table 3, roots exposed to solutions of diuron and linuron obtained after adsorption with AC-C and after adsorption with AC-ZnCl₂ or AC-HNO₃ did not reduce root length, nor did they reduce the rate of cell division or cause significant alterations in cellular number when compared to the control. They were shown to be non-phytotoxic, non-cytotoxic, and non-genotoxic. This result demonstrates the high efficiency of the evaluated adsorbents in removing these herbicides from the aqueous medium.

This study initially aimed to develop an activated carbon from sludge coffee to evaluate the adsorption of various herbicides. The study by Rocha et al. [16] and this one follows the development on a pilot scale. The next steps to be developed are to test the best regeneration cycle for this AC and to carry out prototype tests on a pilot scale to evaluate a possible implementation on an industrial scale. Regarding toxicity, in real-world applications, phytotoxicity, cytotoxicity, and genotoxicity tests should be performed in the same way

as those evaluated in this study. To perform the tests, only 50 mL of each treatment was needed for each onion bulb, and five onion bulbs were used for each treatment. The number of roots and cells analyzed was also the same.

4. Conclusions

The study evaluated diuron and linuron pollutants' percentual removal and toxicity before and after adsorption. Based on the analyzed processes, the removal efficiency values of diuron and linuron with AC-C were similar to those of AC-ZnCl₂. However, AC-ZnCl₂ presented a circular economy solution for the analyzed waste, which is currently discarded without any reuse process.

The adsorption kinetics also showed that the adsorption rate follows the pseudo-first-order and pseudo-second-order models, with adsorption reaching an equilibrium state of adsorption–desorption at around \approx 60 min. Langmuir and Freundlich adsorption isotherms were also evaluated, with the Langmuir model achieving the best fit for diuron, while the Freundlich model was best for linuron.

Finally, ecotoxicity studies in *A. cepa* confirmed the efficiency of pollutant removal in aqueous medium, validating the entire adsorption process used to remove herbicides in aqueous medium.

Author Contributions: Conceptualization, A.P.P., L.B.R., E.B., A.L.R. and O.V.J.; methodology, B.C.d.S.R., L.E.Z.d.M., F.A.O.M. and M.A.N.L.; writing—original draft preparation, A.P.P.; writing—review and editing, A.P.P. and O.V.J. All authors have read and agreed to the published version of the manuscript.

Funding: This research received no external funding.

Data Availability Statement: We declare that all data are in the manuscript. Therefore, the data availability statement does not apply to this study.

Acknowledgments: The authors would like to thank the Multi-User Laboratory at the Londrina Campus, the Multi-User Research Support Laboratory at the Apucarana Campus, the Multi-User Analytical Center and the Multi-User Materials Characterization Center at the Campo Mourão Campus, at the Federal Technological University of Paraná, for supporting the measurements, all campuses of this University located in the state of Paraná-Brazil.

Conflicts of Interest: The authors declare no conflicts of interest.

References

1. Caioni, G.; Merola, C.; Perugini, M.; D'angelo, M.; Cimini, A.M.; Amorena, M.; Benedetti, E. An Experimental Approach to Study the Effects of Realistic Environmental Mixture of Linuron and Propamocarb on Zebrafish Synaptogenesis. *Int. J. Environ. Res. Public Health* **2021**, *18*, 4664. [[CrossRef](#)]
2. Muyaier, T.; Huada, D.R.; Li, W.; Jia, L.; Ross, S.; Des, C.; Cordia, C.; Tri, P.D. Agriculture Development, Pesticide Application and Its Impact on the Environment. *Int. J. Environ. Res. Public Health* **2021**, *18*, 1112. [[CrossRef](#)] [[PubMed](#)]
3. Li, J.; Zhang, W.; Lin, Z.; Huang, Y.; Bhatt, P.; Chen, S. Emerging Strategies for the Bioremediation of the Phenylurea Herbicide Diuron. *Front. Microbiol.* **2021**, *12*, 686509. [[CrossRef](#)] [[PubMed](#)]
4. Agbaogun, B.K.; Fischer, K. Adsorption of Phenylurea Herbicides by Tropical Soils. *Environ. Monit. Assess.* **2020**, *192*, 212. [[CrossRef](#)]
5. Ma, Y.; Pedersen, M.; Vinggaard, A.M. In Vitro Antiandrogenic Effects of the Herbicide Linuron and Its Metabolites. *Chemosphere* **2024**, *349*, 140773. [[CrossRef](#)] [[PubMed](#)]
6. Maharaj, S.; El Ahmadie, N.; Rheingold, S.; El Chehouri, J.; Yang, L.; Souders, C.L.; Martyniuk, C.J. Sub-Lethal Toxicity Assessment of the Phenylurea Herbicide Linuron in Developing Zebrafish (Danio Rerio) Embryo/Larvae. *Neurotoxicol. Teratol.* **2020**, *81*, 106917. [[CrossRef](#)] [[PubMed](#)]
7. Barakan, S.; Aghazadeh, V. The Advantages of Clay Mineral Modification Methods for Enhancing Adsorption Efficiency in Wastewater Treatment: A Review. *Environ. Sci. Pollut. Res.* **2021**, *28*, 2572–2599. [[CrossRef](#)]
8. Wang, H.; Zhang, Z.; Sun, R.; Lin, H.; Gong, L.; Fang, M.; Hu, W.H. HPV Infection and Anemia Status Stratify the Survival of Early T2 Laryngeal Squamous Cell Carcinoma. *J. Voice* **2015**, *29*, 356–362. [[CrossRef](#)]
9. Sultana, M.; Rownok, M.H.; Sabrin, M.; Rahaman, M.H.; Alam, S.M.N. A Review on Experimental Chemically Modified Activated Carbon to Enhance Dye and Heavy Metals Adsorption. *Clean. Eng. Technol.* **2022**, *6*, 100382. [[CrossRef](#)]
10. Boehm, H.P. Surface Oxides on Carbon and Their Analysis: A Critical Assessment. *Carbon* **2002**, *40*, 145–149. [[CrossRef](#)]

11. Boehm, H.P. Some Aspects of the Surface Chemistry of Carbon Blacks and Other Carbons. *Carbon* **1994**, *32*, 759–769. [[CrossRef](#)]
12. Jagadeesh, N.; Sundaram, B. Adsorption of Pollutants from Wastewater by Biochar: A Review. *J. Hazard. Mater. Adv.* **2023**, *9*, 100226. [[CrossRef](#)]
13. Cheng, N.; Wang, B.; Wu, P.; Lee, X.; Xing, Y.; Chen, M.; Gao, B. Adsorption of Emerging Contaminants from Water and Wastewater by Modified Biochar: A Review. *Environ. Pollut.* **2021**, *273*, 116448. [[CrossRef](#)] [[PubMed](#)]
14. Saberian, M.; Li, J.; Donnoli, A.; Bonderenko, E.; Oliva, P.; Gill, B.; Lockrey, S.; Siddique, R. Recycling of Spent Coffee Grounds in Construction Materials: A Review. *J. Clean. Prod.* **2021**, *289*, 125837. [[CrossRef](#)]
15. Siregar, C.A.; Siregar, A.M.; Lubis, R.W.; Marpaung, D. Rancang Bangun Mesin Giling Kopi Untuk Menunjang Dan Membuka Unit Usaha Baru Mitra Deli Coffe. *ABDI SABHA (J. Pengabd. Kpd. Masy.)* **2022**, *3*, 174–180. [[CrossRef](#)]
16. da S. Rocha, B.C.; de Moraes, L.E.Z.; Santo, D.E.; Peron, A.P.; de Souza, D.C.; Bona, E.; Valarini, O. Removal of Bentazone Using Activated Carbon from Spent Coffee Grounds. *J. Chem. Technol. Biotechnol.* **2024**, *99*, 1342–1355. [[CrossRef](#)]
17. Javier Sánchez, A. Characterization of Activated Carbon Produced from Coffee Residues by Chemical and Physical Activation. *KTH Chem. Sci. Eng.* **2011**, *66*, 14–28.
18. Jagdale, P.; Ziegler, D.; Rovere, M.; Tulliani, J.M.; Tagliaferro, A. Waste Coffee Ground Biochar: A Material for Humidity Sensors. *Sensors* **2019**, *19*, 801. [[CrossRef](#)]
19. Fernandes, A.S.; Mello, F.V.C.; Thode Filho, S.; Carpes, R.M.; Honório, J.G.; Marques, M.R.C.; Felzenszwalb, I.; Ferraz, E.R.A. Impacts of Discarded Coffee Waste on Human and Environmental Health. *Ecotoxicol. Environ. Saf.* **2017**, *141*, 30–36. [[CrossRef](#)]
20. Ferraz, F.M.; Yuan, Q. Organic Matter Removal from Landfill Leachate by Adsorption Using Spent Coffee Grounds Activated Carbon. *Sustain. Mater. Technol.* **2020**, *23*, e00141. [[CrossRef](#)]
21. Milanković, V.; Tasić, T.; Brković, S.; Potkonjak, N.; Unterweger, C.; Bajuk-Bogdanović, D.; Pašti, I.; Lazarević-Pašti, T. Spent Coffee Grounds-Derived Carbon Material as an Effective Adsorbent for Removing Multiple Contaminants from Wastewater: A Comprehensive Kinetic, Isotherm, and Thermodynamic Study. *J. Water Process Eng.* **2024**, *63*, 105507. [[CrossRef](#)]
22. Milanković, V.; Tasić, T.; Pejčić, M.; Pašti, I.; Lazarević-Pašti, T. Spent Coffee Grounds as an Adsorbent for Malathion and Chlorpyrifos—Kinetics, Thermodynamics, and Eco-Neurotoxicity. *Foods* **2023**, *12*, 2397. [[CrossRef](#)] [[PubMed](#)]
23. Rosson, E.; Garbo, F.; Marangoni, G.; Bertani, R.; Lavagnolo, M.C.; Moretti, E.; Talon, A.; Mozzon, M.; Sgarbossa, P. Activated Carbon from Spent Coffee Grounds: A Good Competitor of Commercial Carbons for Water Decontamination. *Appl. Sci.* **2020**, *10*, 5598. [[CrossRef](#)]
24. Zbair, M.; El Hadrami, A.; Bellarbi, A.; Monkade, M.; Zradba, A.; Brahmi, R. Herbicide Diuron Removal from Aqueous Solution by Bottom Ash: Kinetics, Isotherm, and Thermodynamic Adsorption Studies. *J. Environ. Chem. Eng.* **2020**, *8*, 103667. [[CrossRef](#)]
25. Georgin, J.; Franco, D.S.P.; Netto, M.S.; Gama, B.M.V.; Fernandes, D.P.; Sepúlveda, P.; Silva, L.F.O.; Meili, L. Effective Adsorption of Harmful Herbicide Diuron onto Novel Activated Carbon from *Hovenia Dulcis*. *Colloids Surfaces A Physicochem. Eng. Asp.* **2022**, *654*, 129900. [[CrossRef](#)]
26. Vieira, Y.; Silveira, J.P.; Dotto, G.L.; Knani, S.; Vieillard, J.; Georgin, J.; Franco, D.S.P.; Lima, E.C. Mechanistic Insights and Steric Interpretations through Statistical Physics Modelling and Density Functional Theory Calculations for the Adsorption of the Pesticides Atrazine and Diuron by *Hovenia Dulcis* Biochar. *J. Mol. Liq.* **2022**, *367*, 120418. [[CrossRef](#)]
27. Georgin, J.; Pinto, D.; Franco, D.S.P.; Schadeck Netto, M.; Lazarotto, J.S.; Allasia, D.G.; Tassi, R.; Silva, L.F.O.; Dotto, G.L. Improved Adsorption of the Toxic Herbicide Diuron Using Activated Carbon Obtained from Residual Cassava Biomass (*Manihot esculenta*). *Molecules* **2022**, *27*, 7574. [[CrossRef](#)]
28. Asgari, G.; Abdipour, H.; Shadjou, A.M. A Review of Novel Methods for Diuron Removal from Aqueous Environments. *Heliyon* **2023**, *9*, e23134. [[CrossRef](#)]
29. Elazabi, M.; Draskovic, B.; Novakovic, M.; Mihajlovic, I.; Hgeig, A. Adsorption of Linuron and Isoproturon Pesticides on Commercial Activated Carbon, Norit SA2. *Fresenius Environ. Bull.* **2021**, *30*, 1030–1043.
30. Sirival, R.; Patdhanagul, N.; Preecharram, S.; Nantaphan, P.; Mahem, R. The Performance of Synthetic Zeolite Combined with Activated Carbon for Removal of Linuron Herbicide. *Suranaree J. Sci. Technol.* **2020**, *27*, 030027-1–030027-5.
31. Yang, J.; Sun, H.; Liu, Y.; Wang, X.; Valizadeh, K. The Sorption of Tebuconazole and Linuron from an Aqueous Environment with a Modified Sludge-Based Biochar: Effect, Mechanisms, and Its Persistent Free Radicals Study. *J. Chem.* **2021**, *2021*, 2912054. [[CrossRef](#)]
32. Belaroui, L.S.; Ouali, A.; Bengueddach, A.; Lopez Galindo, A.; Peña, A. Adsorption of Linuron by an Algerian Palygorskite Modified with Magnetic Iron. *Appl. Clay Sci.* **2018**, *164*, 26–33. [[CrossRef](#)]
33. Rissouli, L.; Benicha, M.; Chabbi, M. Contribution to the Elimination of Linuron by the Adsorption Process Using Chitin and Chitosan Biopolymers. *J. Mater. Environ. Sci.* **2016**, *7*, 531–540.
34. El-Nahhal, Y.; Abadsa, M.; Affifi, S. Adsorption of Diuron and Linuron in Gaza Soils. *Am. J. Anal. Chem.* **2013**, *04*, 94–99. [[CrossRef](#)]
35. Debien, I.C.N.; Vardanega, R.; Santos, D.T.; Meireles, M.A.A. Pressurized Liquid Extraction as a Promising and Economically Feasible Technique for Obtaining Beta-Ecdysone-Rich Extracts from Brazilian Ginseng (*Pfaffia glomerata*) Roots. *Sep. Sci. Technol.* **2015**, *50*, 1647–1657. [[CrossRef](#)]
36. Dean, J.R. Pressurized Liquid Extraction. In *Extraction Techniques for Environmental Analysis*; Wiley: Hoboken, NJ, USA, 2022; pp. 171–204. [[CrossRef](#)]

37. Haro, N.K.; Dávila, I.V.J.; Nunes, K.G.P.; de Franco, M.A.E.; Marcilio, N.R.; Féris, L.A. Kinetic, Equilibrium and Thermodynamic Studies of the Adsorption of Paracetamol in Activated Carbon in Batch Model and Fixed-Bed Column. *Appl. Water Sci.* **2021**, *11*, 38. [[CrossRef](#)]
38. Milonjić, S.K.; Kopečni, M.M.; Ilić, Z.E. The Point of Zero Charge and Adsorption Properties of Natural Magnetite. *J. Radioanal. Chem.* **1983**, *78*, 15–24. [[CrossRef](#)]
39. Gonçalves Júnior, D.R.; de Araújo, P.C.C.; Simões, A.L.G.; Voll, F.A.P.; Parizi, M.P.S.; de Oliveira, L.H.; Ferreira-Pinto, L.; Cardozo-Filho, L.; de Jesus Santos, E. Assessment of the Adsorption Capacity of Phenol on Magnetic Activated Carbon. *Asia-Pacific J. Chem. Eng.* **2022**, *17*, e2725. [[CrossRef](#)]
40. Tan, K.L.; Hameed, B.H. Insight into the Adsorption Kinetics Models for the Removal of Contaminants from Aqueous Solutions. *J. Taiwan Inst. Chem. Eng.* **2017**, *74*, 25–48. [[CrossRef](#)]
41. Karri, R.R.; Sahu, J.N.; Jayakumar, N.S. Optimal Isotherm Parameters for Phenol Adsorption from Aqueous Solutions onto Coconut Shell Based Activated Carbon: Error Analysis of Linear and Non-Linear Methods. *J. Taiwan Inst. Chem. Eng.* **2017**, *80*, 472–487. [[CrossRef](#)]
42. Fiskesjö, G. The Allium Test as a Standard in Environmental Monitoring. *Hereditas* **1985**, *102*, 99–112. [[CrossRef](#)] [[PubMed](#)]
43. Kruskal, W.H.; Wallis, W.A. Use of Ranks in One-Criterion Variance Analysis. *J. Am. Stat. Assoc.* **1952**, *47*, 583–621. [[CrossRef](#)]
44. Mrozik, W.; Minofar, B.; Thongsamer, T.; Wiriyaphong, N.; Khawkomol, S.; Plaimart, J.; Vakros, J.; Karapanagioti, H.; Vinitnatharat, S.; Werner, D. Valorisation of Agricultural Waste Derived Biochars in Aquaculture to Remove Organic Micropollutants from Water—Experimental Study and Molecular Dynamics Simulations. *J. Environ. Manag.* **2021**, *300*, 113717. [[CrossRef](#)] [[PubMed](#)]
45. Amin, F.R.; Huang, Y.; He, Y.; Zhang, R.; Liu, G.; Chen, C. Biochar Applications and Modern Techniques for Characterization. *Clean Technol. Environ. Policy* **2016**, *18*, 1457–1473. [[CrossRef](#)]
46. Fletcher, A.; Somorin, T.; Aladeokin, O. Production of High Surface Area Activated Carbon from Peanut Shell by Chemical Activation with Zinc Chloride: Optimisation and Characterization. *Bioenergy Res.* **2024**, *17*, 467–478. [[CrossRef](#)]
47. Heidarinejad, Z.; Dehghani, M.H.; Heidari, M.; Javedan, G.; Ali, I.; Sillanpää, M. Methods for Preparation and Activation of Activated Carbon: A Review. *Environ. Chem. Lett.* **2020**, *18*, 393–415. [[CrossRef](#)]
48. Anisuzzaman, S.M.; Joseph, C.G.; Krishnaiah, D.; Bono, A.; Suali, E.; Abang, S.; Fai, L.M. Removal of Chlorinated Phenol from Aqueous Media by Guava Seed (*Psidium guajava*) Tailored Activated Carbon. *Water Resour. Ind.* **2016**, *16*, 29–36. [[CrossRef](#)]
49. Gundogdu, A.; Duran, C.; Senturk, H.B.; Soylak, M.; Imamoglu, M.; Onal, Y. Physicochemical Characteristics of a Novel Activated Carbon Produced from Tea Industry Waste. *J. Anal. Appl. Pyrolysis* **2013**, *104*, 249–259. [[CrossRef](#)]
50. Chen, W.S.; Chen, Y.C.; Lee, C.H. Modified Activated Carbon for Copper Ion Removal from Aqueous Solution. *Processes* **2022**, *10*, 150. [[CrossRef](#)]
51. Ternero-Hidalgo, J.J.; Rosas, J.M.; Palomo, J.; Valero-Romero, M.J.; Rodríguez-Mirasol, J.; Cordero, T. Functionalization of Activated Carbons by HNO₃ Treatment: Influence of Phosphorus Surface Groups. *Carbon N. Y.* **2016**, *101*, 409–419. [[CrossRef](#)]
52. Grilla, E.; Vakros, J.; Konstantinou, I.; Manariotis, I.D.; Mantzavinos, D. Activation of Persulfate by Biochar from Spent Malt Rootlets for the Degradation of Trimethoprim in the Presence of Inorganic Ions. *J. Chem. Technol. Biotechnol.* **2020**, *95*, 2348–2358. [[CrossRef](#)]
53. Giannakopoulos, S.; Frontistis, Z.; Vakros, J.; Pouloupoulos, S.G.; Manariotis, I.D.; Mantzavinos, D. Combined Activation of Persulfate by Biochars and Artificial Light for the Degradation of Sulfamethoxazole in Aqueous Matrices. *J. Taiwan Inst. Chem. Eng.* **2022**, *136*, 104440. [[CrossRef](#)]
54. do Nascimento, R.F.; de Lima, A.C.A.; Vidal, C.B.; de Melo, D.Q.; Raulino, G.S.C. *Adsorção: Aspectos Teóricos e Aplicações Ambientais*; Imprensa Universitária: Fortaleza, Brazil, 2020; Volume 308.
55. Benaouda, B.; Iman, G.; Michalkiewicz, B. Study on Anionic Dye Toxicity Reduction from Simulated Media by MnO₂/Agro-Biomass Based-AC Composite Adsorbent. *Ind. Crops Prod.* **2024**, *208*, 117789. [[CrossRef](#)]
56. Liu, Y.; Shen, L. From Langmuir Kinetics to First- and Second-Order Rate Equations for Adsorption. *Langmuir* **2008**, *24*, 11625–11630. [[CrossRef](#)]
57. McCabe, W.C.; Smith, J.C.; Harriot, P. Unit Operations of Chemical Engineering. *Choice Rev. Online* **1993**, *30*, 30-6200. [[CrossRef](#)]
58. Wang, T.; Zhai, Y.; Zhu, Y.; Li, C.; Zeng, G. A Review of the Hydrothermal Carbonization of Biomass Waste for Hydrochar Formation: Process Conditions, Fundamentals, and Physicochemical Properties. *Renew. Sustain. Energy Rev.* **2018**, *90*, 223–247. [[CrossRef](#)]
59. da Rocha, S.A.F.; da Rocha, B.C.S.; de Moraes, L.E.Z.; Villaça, J.M.P.; Scapin, D.; Santo, D.E.; da Gonzalez, R.; Junior, O.V.; Peron, A.P. Evaluation and Simulation of the Adsorption Capacity of Octocrylene Sunscreen on Commercial Carbon and Biochar from Spent Coffee Beans. *Processes* **2024**, *12*, 1249. [[CrossRef](#)]
60. Taamalli, A.; Arráez-Román, D.; Barrajon-Catalán, E.; Ruiz-Torres, V.; Pérez-Sánchez, A.; Herrero, M.; Ibañez, E.; Micol, V.; Zarrouk, M.; Segura-Carretero, A.; et al. Use of Advanced Techniques for the Extraction of Phenolic Compounds from Tunisian Olive Leaves: Phenolic Composition and Cytotoxicity against Human Breast Cancer Cells. *Food Chem. Toxicol.* **2012**, *50*, 1817–1825. [[CrossRef](#)]
61. Santo, D.E.; Dusman, E.; da Silva Gonzalez, R.; Romero, A.L.; dos Santos Gonçalves do Nascimento, G.C.; de Souza Moura, M.A.; Bressiani, P.A.; Filipi, Á.C.K.; Gomes, E.M.V.; Pokrywiecki, J.C.; et al. Prospecting Toxicity of Octocrylene in *Allium cepa* L. and *Eisenia Fetida* Sav. *Environ. Sci. Pollut. Res.* **2023**, *30*, 8257–8268. [[CrossRef](#)]

62. Frâncica, L.S.; Gonçalves, E.V.; Santos, A.A.; Vicente, Y.S.; Silva, T.S.; Gonzalez, R.S.; Almeida, P.M.; Feitoza, L.L.; Bueno, P.A.A.; Souza, D.C.; et al. Antiproliferative, Genotoxic and Mutagenic Potential of Synthetic Chocolate Food Flavoring. *Brazilian J. Biol.* **2022**, *82*, e243628. [[CrossRef](#)]
63. Federico, C.; Palmieri, C.; Pappalardo, A.M.; Ferrito, V.; Pappalardo, M.; Librando, V.; Saccone, S. Mutagenic Properties of Linuron and Chlorbromuron Evaluated by Means of Cytogenetic Biomarkers in Mammalian Cell Lines. *Environ. Sci. Pollut. Res.* **2016**, *23*, 17018–17025. [[CrossRef](#)] [[PubMed](#)]
64. Basal, W.T.; Ahmed, A.R.T.; Mahmoud, A.A.; Omar, A.R. Lufenuron Induces Reproductive Toxicity and Genotoxic Effects in Pregnant Albino Rats and Their Fetuses. *Sci. Rep.* **2020**, *10*, 19544. [[CrossRef](#)] [[PubMed](#)]
65. Topal, A.; Gergit, A.; Özkaraca, M. Assessment of Oxidative DNA Damage, Oxidative Stress Responses and Histopathological Alterations in Gill and Liver Tissues of *Oncorhynchus mykiss* Treated with Linuron. *Hum. Exp. Toxicol.* **2021**, *40*, 1112–1121. [[CrossRef](#)]
66. Ergin, T.; Inceer, H.; Ergin, B. Investigation of Antimutagenic Effect of *Rosa canina* L. Against Linuron Induced DNA Damage on Root Meristematic Cells of *Allium cepa* L. *Cytologia* **2020**, *85*, 233–237. [[CrossRef](#)]
67. Akcha, F.; Spagnol, C.; Rouxel, J. Genotoxicity of Diuron and Glyphosate in Oyster Spermatozoa and Embryos. *Aquat. Toxicol.* **2012**, *106–107*, 104–113. [[CrossRef](#)]
68. Behrens, D.; Rouxel, J.; Burgeot, T.; Akcha, F. Comparative Embryotoxicity and Genotoxicity of the Herbicide Diuron and Its Metabolites in Early Life Stages of *Crassostrea Gigas*: Implication of Reactive Oxygen Species Production. *Aquat. Toxicol.* **2016**, *175*, 249–259. [[CrossRef](#)]
69. Sharma, S.; Vig, A. Genotoxicity of Atrazine, Avenoxan, Diuron and Quizalofop-P-Ethyl Herbicides Using the *Allium cepa* Root Chromosomal Aberration Assay. *Terr. Aquat. Environ. Toxicol.* **2012**, *6*, 90–95.
70. Peraza-Vega, R.I.; Castañeda-Sortibrán, A.N.; Valverde, M.; Rojas, E.; Rodríguez-Arnaiz, R. Assessing Genotoxicity of Diuron on *Drosophila Melanogaster* by the Wing-Spot Test and the Wing Imaginal Disk Comet Assay. *Toxicol. Ind. Health* **2017**, *33*, 443–453. [[CrossRef](#)]

Disclaimer/Publisher’s Note: The statements, opinions and data contained in all publications are solely those of the individual author(s) and contributor(s) and not of MDPI and/or the editor(s). MDPI and/or the editor(s) disclaim responsibility for any injury to people or property resulting from any ideas, methods, instructions or products referred to in the content.